Transmission Electron Microscopic Observations of Mechanical Twinning in Metastable Beta Titanium Alloys

S. HANADA and O. IZUMI

Microstructure and crystallography of a stress-induced plate in metastable β titanium alloys, Ti-V, Ti-Mo, Ti-Nb, Ti-Fe, were investigated by a combination of two surface trace analysis and transmission electron microscopy. Stress-induced ω phase transformation or $\{332\}\langle 113\rangle$ twinning appeared in circumstances where β phase was very unstable. It was found that there were two types of $\{332\}\langle 113\rangle$ twinning, depending on whether one variant of ω phase was preferentially induced in a twin or not. Stress-induced ω phase not relating to $\{332\}\langle 113\rangle$ twinning was not observed in matrix. This suggests that stress-induced ω phase transformation is accompanied with $\{332\}\langle 113\rangle$ twinning. Preferential formation of one ω variant was influenced not only by alloy system and its composition, but also by cooling rate from solution treatment temperature. The relation between athermal ω structure and stress-induced ω phase transformation or plastic deformation mode is also discussed.

I. INTRODUCTION

THERE are two general types of equilibrium phase diagrams of titanium based transition metal alloys in which omega phase (hexagonal) can be formed,[1] *i.e.*, β-isomorphous alloys such as Ti-V, Ti-Mo, and Ti-Nb, and β-eutectoid alloys such as Ti-Fe and Ti-Cr as shown in Figure 1. In both types of β titanium alloys (bcc), deformation at room temperature has recently been shown to produce $\{332\}\langle 113\rangle$ twinning under certain circumstances.[2,3,4] The $\{332\}\langle 113\rangle$ twinning is found in the shaded region of the diagrams, as schematically shown in Figure 1, where Ms indicates martensitic start temperature. It is apparent from this figure that the twinning occurs in a metastable β phase region close to the Ms curve. β phase in the region always contains athermal ω phase introduced during quenching, and the retained β phase decomposes into isothermal ω phase during aging at relatively low temperature above room temperature. Therefore, β phase close to Ms curve is thought to be unstable at room temperature. Oka and Taniguchi[5] have suggested that instability of β phase is favorable for producing $\{332\}\langle 113\rangle$ twinning under deformation, since in the $\{332\}\langle 113\rangle$ twinning mode presented by Crocker[6] one-half of the atoms must shuffle into the direction different from that of the twinning shear so as to settle in right lattice points.

On the other hand, deformation at room temperature has been reported to induce ω phase in various β titanium alloys. Bagaryatskij *et al.*[7] found that ω phase formed during deformation of quenched Ti-8 wt pct Cr alloy. Kuan *et al.*[8] showed that one variant ω phase was induced during deformation of quenched Ti-15.8 wt pct V and Ti-20 wt pct V alloy single crystals. Wood[9] reported that ω phase in a quenched Ti-15 wt pct Mo alloy formed in greater quantities as cold deformation proceeded. Hida *et al.*[10] also showed that ω phase was induced by deformation of a quenched Ti-14 wt pct Mo alloy single crystal. Luhman and Curzon[11] have observed that deformation of a vacuum cooled Ti-35.4 wt pct Nb alloy leads to anisotropic population of four variants of ω phase. It is noticed from those

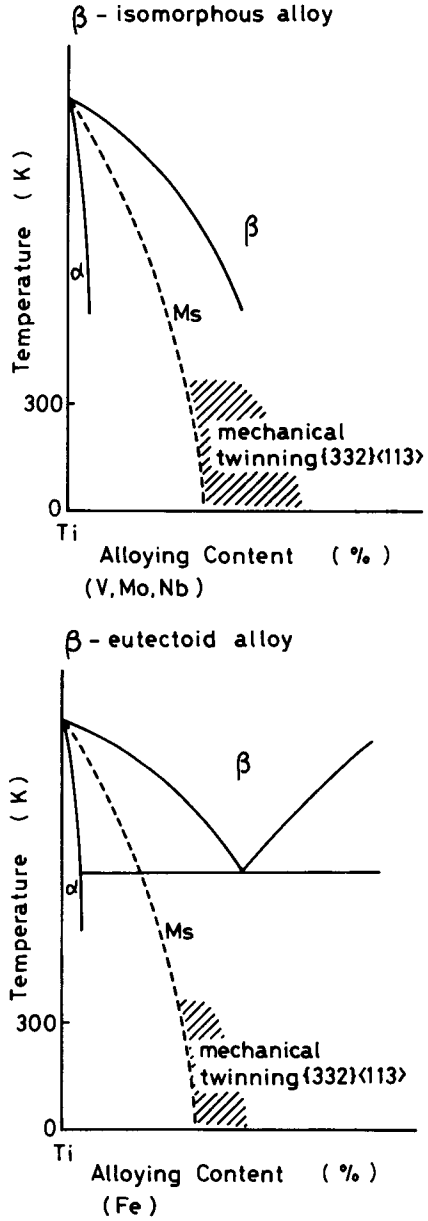

Fig. 1—Typical phase diagrams for titanium alloy systems in which ω phase can be formed. The shaded region indicates circumstances where $\{332\}\langle 113\rangle$ mechanical twinning or stress-induced ω transformation occurs.

S. HANADA, Instructor, and O. IZUMI, Professor, are with The Research Institute for Iron, Steel and Other Metals, Tohoku University, 2-1-1, Katahira, Sendai 980, Japan.

Manuscript submitted July 11, 1985.

publications that the solute content of the alloys is close to the lower limit for the retention of β phase, and therefore it falls on composition in which $\{332\}\langle 113\rangle$ twinning has been found in Figure 1.

No information, however, is available on the relation between $\{332\}\langle 113\rangle$ twinning and ω phase formation of metastable β phase titanium alloys under deformation. The objective of the present study is to provide information on this relation.

II. EXPERIMENTAL

Ti-16, 18, 20, 22, 24, 26, 27, 28 wt pct V alloys and Ti-11, 12, 13, 15, 18, 20 wt pct Mo alloys were prepared by arc melting in an argon atmosphere. The arc-melted buttons were homogenized at 1373 K for 43 ks under a vacuum of about 10^{-4} Pa. Single crystals were grown using an electron beam zone melting apparatus under a vacuum of 3×10^{-5} Pa. Single crystal specimens for compressive and tensile tests with dimensions of 2.7 mm × 2.7 mm × 6 mm and 2.7 mm × 2.7 mm × 20 mm, respectively, were prepared by spark cutting. Ti-36, 40, 42, 46, 52 wt pct Nb alloys were arc melted in an argon atmosphere. 4 mm thick plates were made by cold rolling of the arc-melted buttons (approximately 10 mm in thickness) and annealed under a vacuum of 8×10^{-5} Pa at 1673 K for 36 ks to remove solute segregation introduced during solidification. The annealed plates were again cold rolled to 2.5 mm in thickness and cut to slices of 2.5 mm in width. The bars with a square cross section of 2.5 mm × 2.5 mm were annealed at 1672 K for 3.6 ks under a vacuum of 8×10^{-5} Pa. Single crystal compressive samples of 2.5 mm × 2.5 mm × 6 mm were obtained from the annealed bars with bamboo structure by means of a spark cutting machine. Ti-4, 4.5, 5, 6, 10 wt pct Fe alloys were prepared by arc melting in an argon atmosphere. The arc-melted buttons were hot-rolled at 1200 K to 3 mm thick plates. Bars with a square cross section of 2.5 mm × 2.5 mm were obtained from the plates by cutting and grinding and subjected to annealing for 36 ks at 1473 K for grain growth. Single crystal compressive samples of 2.5 mm × 2.5 mm × 5 mm were spark cut from the bars. Ti-15 wt pct Mo-5 wt pct Zr and Ti-15 wt pct Mo-5 wt pct Zr-3 wt pct Al alloys kindly supplied by Kobe Steel, Ltd. were strain-annealed at 1673 K for 36 ks. Single crystal compressive samples were spark cut from the large grained alloys.

The samples of Ti-V, Ti-Mo, Ti-Nb, Ti-Fe, Ti-Mo-Zr, and Ti-Mo-Zr-Al alloys were sealed in a vacuum quartz tube after chemical polishing to remove surface damage introduced by spark cutting. They were homogenized at 1273 K for 3.6 ks and quenched into ice water. After mechanical and chemical polishing, the samples were deformed at 300 K using an Instron type testing machine. Deformation mode at an initial stage, usually less than 2 pct strain, was determined by two surface trace analysis and transmission electron microscopy techniques. For example, when an interface plane of a stress-induced plate determined by two surface trace analysis was $(\bar{3}32)$, a thin foil parallel to (110) plane of undeformed matrix was prepared, since the electron beam in the [110] direction of the β matrix is also in the [110] direction of the $(\bar{3}32)[\bar{1}1\bar{3}]$ twin. Thus, the occurrence of $(\bar{3}32)[\bar{1}1\bar{3}]$ twinning can be easily checked by the diffraction pattern taken from a boundary region of the stress-induced plate.

III. RESULTS

A. *Ti-V Alloys*

It has been reported that β phase of Ti-V alloys is retained in higher solute content than 15.5 wt pct V and deformation at room temperature of the metastable β phase results in induction of either ω transformation[8] or $\{332\}\langle 113\rangle$ twinning in Ti-V alloys containing 16 ~ 22 wt pct V.[2,5] Therefore, Ti-16 to 22 wt pct V single crystals were slightly deformed, and the crystals were observed by transmission electron microscopy. Slip and stress-induced plates were observed in Ti-22 wt pct V dependent on orientation in agreement with previous work.[2] Figure 2 shows a bright-field image of the boundary of a stress-induced plate in deformed Ti-22 wt pct V. The observed foil was parallel to (110) and perpendicular to $(\bar{3}32)$, since the interface plane determined by two surface trace analyses was $(\bar{3}32)$. A high density of dislocations, composed of straight dislocations along $[\bar{1}11]$ of the plate as well as tangled dislocations, is observed in the plate. Boundaries of stress-induced plates were usually seen to be straight and correspond with $[\bar{1}1\bar{3}]$, but it sometimes deviated from the direction. Figures 3(a), (b), and (c) show electron diffraction patterns obtained from the boundary region in Figure 2, the matrix and plate adjacent to the boundary, respectively. Figure 3(a) can be indexed as the matrix of β phase containing athermal ω phase and its twin, as shown in Figure 4. When the electron beam is in the [110] direction of the β matrix, some of the reflections arising from the two variants among four variants in ω phase appear without being obscured by the matrix spots. It is clearly seen in Figures 3(b) and (c) that reflections of the two ω phase variants have the equal intensity in the matrix and twin. Figure 5 shows the result of deformed Ti-18 wt pct V, where the foil was prepared in a similar manner to that in Figure 2. A high density of dislocations along $[\bar{1}1\bar{1}]$ is visible in the plate. Dislocations were hardly observed in the

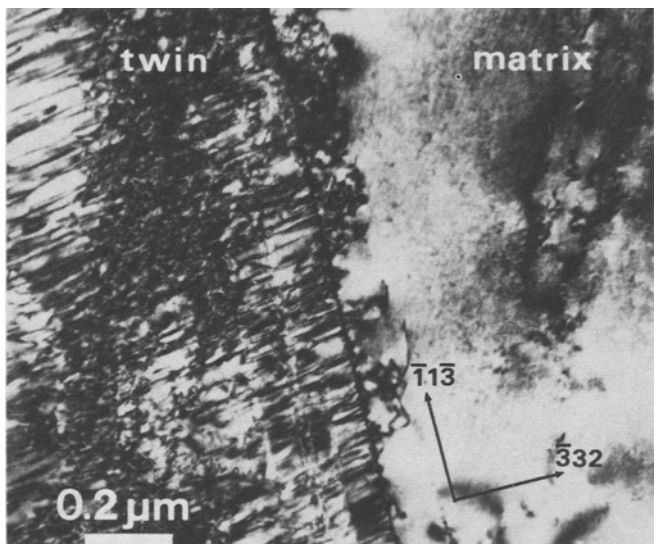

Fig. 2—Bright-field image of a $(\bar{3}32)[\bar{1}1\bar{3}]$ twin boundary in Ti-22 wt pct V.

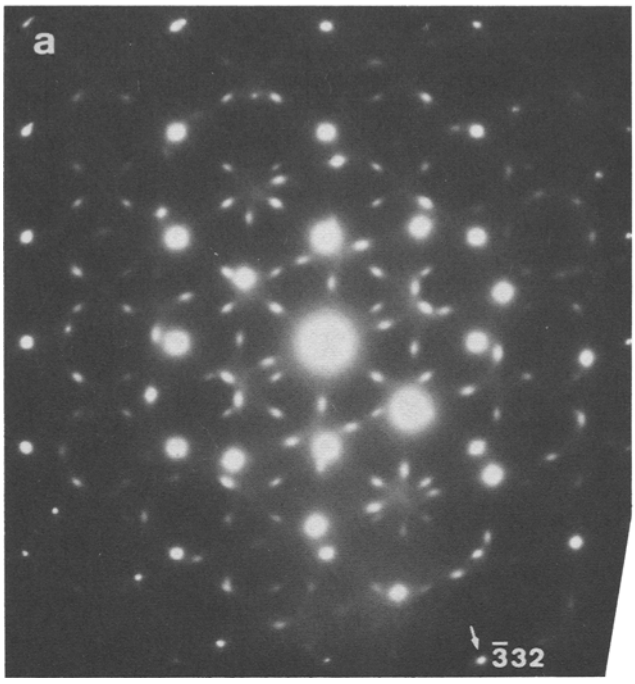

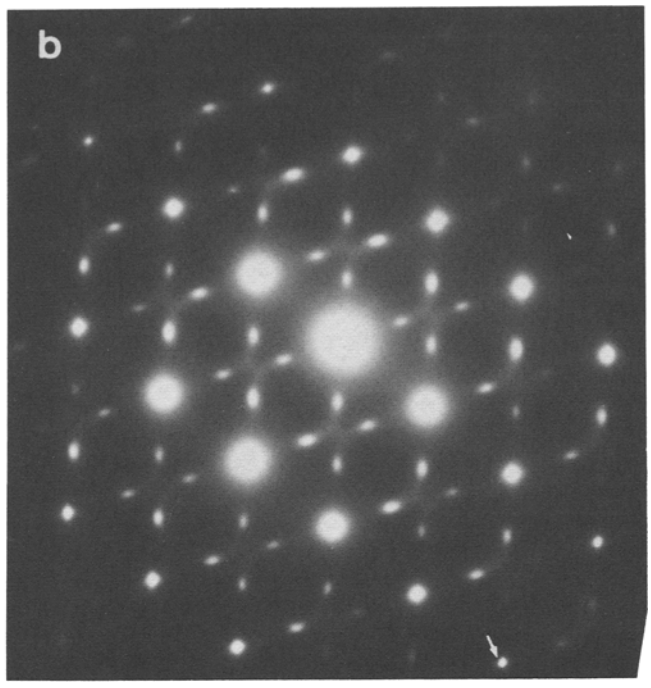

Fig. 3—Electron diffraction patterns from the $(\bar{3}32)[\bar{1}1\bar{3}]$ twin boundary region (*a*), matrix (*b*), and twin (*c*) in Ti-22 wt pct V. The electron beam $\| [110]_\beta$.

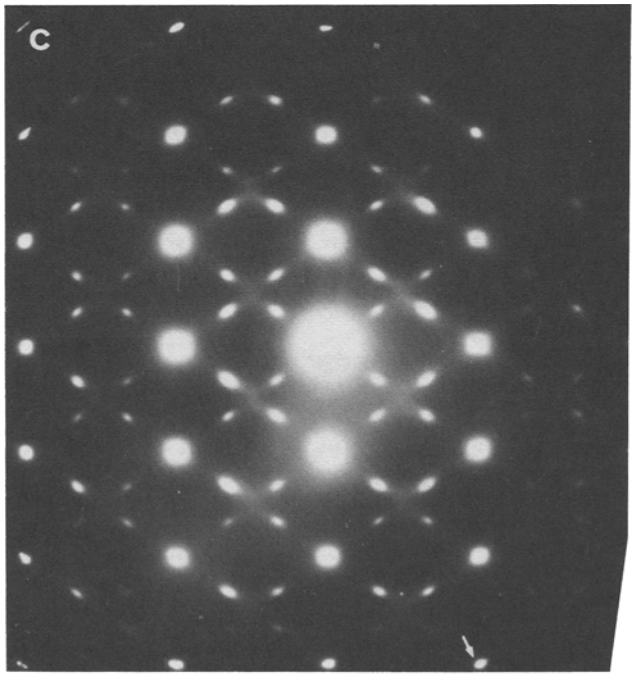

matrix, but mottled contrast was always present, indicating that the amount of athermal ω phase increased with decreasing vanadium content. Figures 6(a), (b), and (c) show electron diffraction patterns obtained from the boundary region in Figure 5, the matrix and plate adjacent to the boundary, respectively. By considering Figures 6(b) and (c), the reflections in Figure 6(a), can be explained as arising from the matrix and single variant ω_2 of Figure 4. Neither β nor ω_1 phase reflections are seen in the plate. The same result as Figure 6 was obtained in Ti-16 and 20 wt pct V. Thus, we can say that deformation at room temperature in Ti-16 to 20 wt pct V results in single variant ω

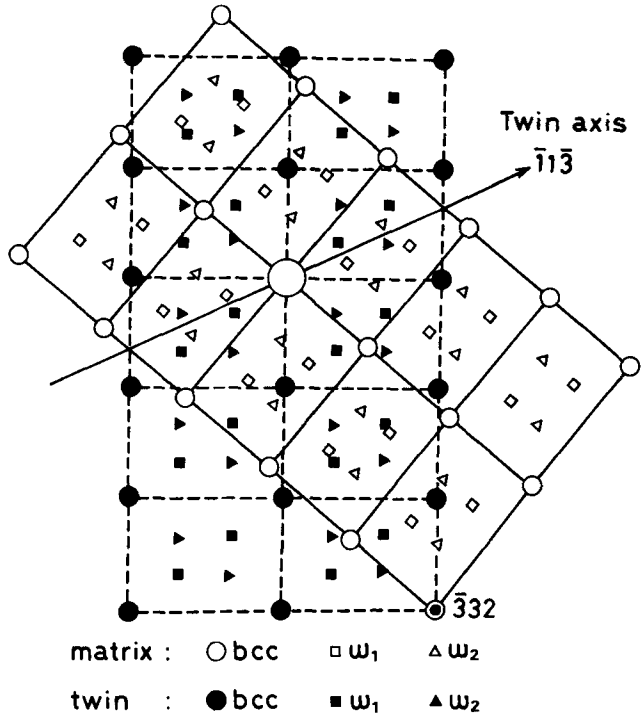

Fig. 4—Schematic diffraction pattern used to interpret Fig. 3(a).

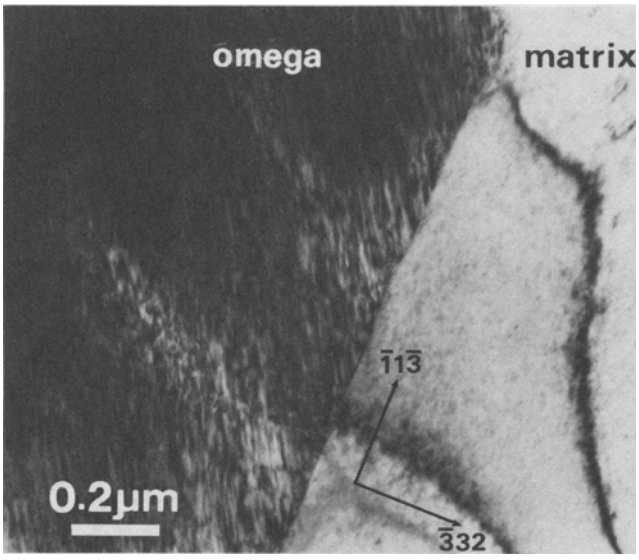

Fig. 5—Bright-field image of a stress-induced ω plate boundary in Ti-18 wt pct V.

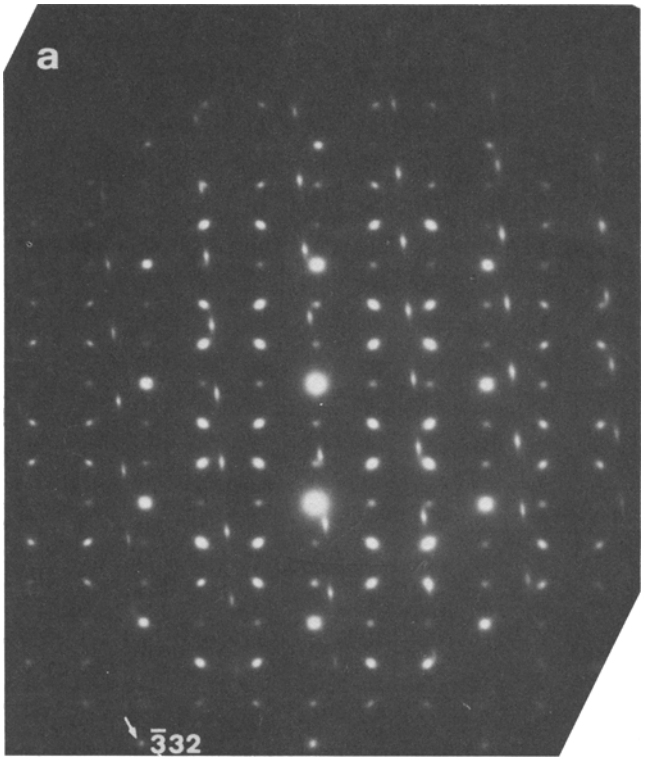

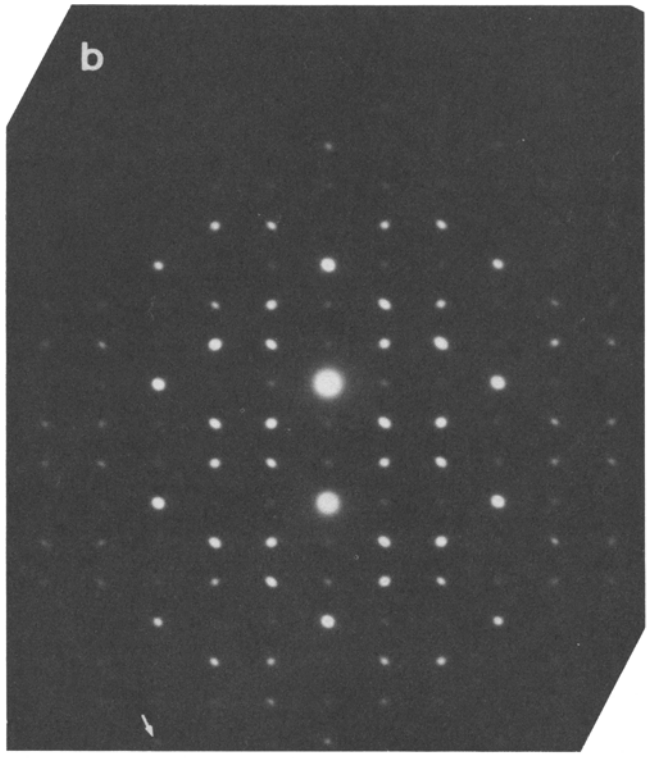

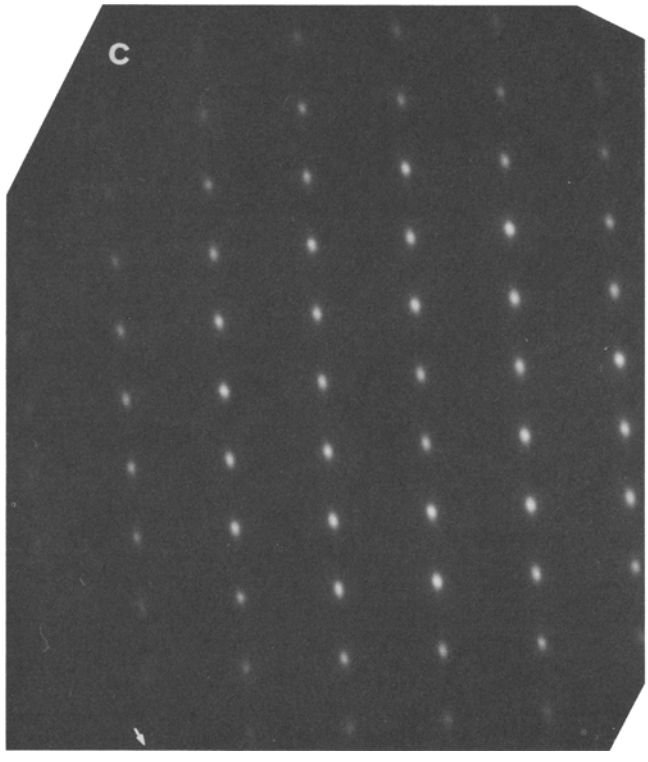

Fig. 6—Electron diffraction patterns from the boundary region of the stress-induced ω plate (*a*), matrix (*b*), and plate (*c*) in Ti-18 wt pct V. The electron beam $\|[110]_\beta$.

phase transformation *via* {332}⟨113⟩ twinning. Only slip occurred in Ti-V alloys containing more than 24 wt pct V. In order to interpret the composition dependence of plastic deformation mode, electron diffraction patterns of as-quenched alloys were investigated as a function of position of ω reflections. Figure 7 shows $(110)_\beta$ diffraction patterns in Ti-18 and 24 wt pct V. It is seen that ω reflections become diffuse as vanadium content increases and the 0002 reflection in Ti-24 wt pct V is displaced toward 0001, away from the position expected for the ideal ω structure, although that in Ti-18 wt pct V is not. The displacement means that the ratio of reciprocal distance d^*_{0002}/d^*_{222} is not equal to 0.667. The obtained results on the ratio in Ti-V alloys are summarized in Figure 8. It is likely that the ratio is related to plastic deformation mode as follows. The displacement is not present in vanadium content less than 22 wt pct, where stress-induced ω phase transformation is observed. At small displacement such as in Ti-22 wt pct V, deformation leads to {332}⟨113⟩ twinning which does not induce ω phase transformation, while at large displacement it results in slip only. It is noted from Figure 8 that the displacement increases continuously with increasing vanadium content. For reference d^*_{0002}/d^*_{222} of Ti-50 wt pct V was measured by using broadened ω phase reflections, usually called diffuse scattering. The ratio is 0.630 and seems to fall on a value extrapolated from Figure 8.

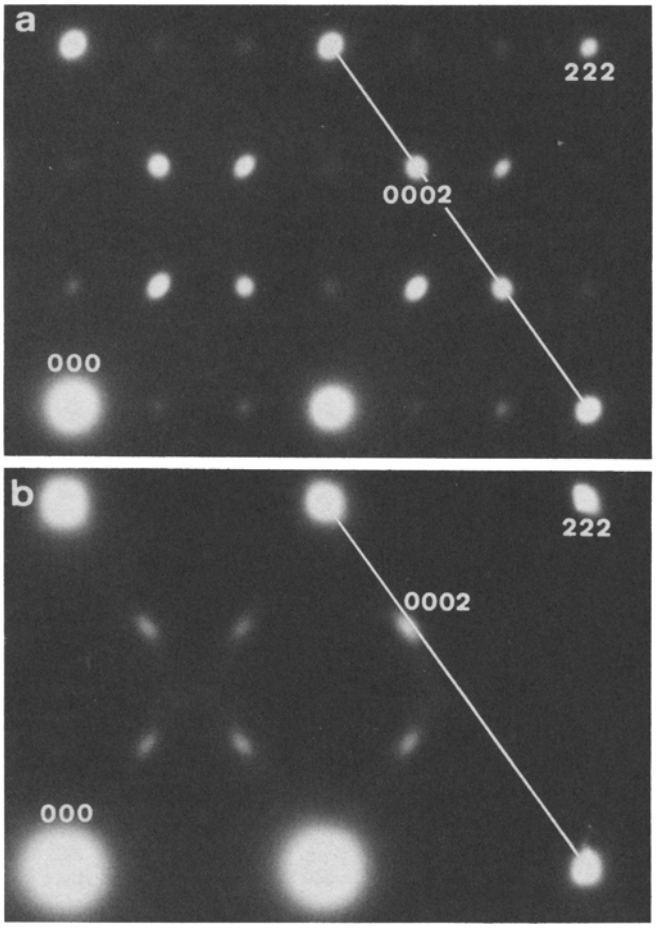

Fig. 7—Electron diffraction patterns from as-quenched Ti-18 wt pct V (*a*) and Ti-24 wt pct V (*b*). The electron beam ∥ $[110]_\beta$.

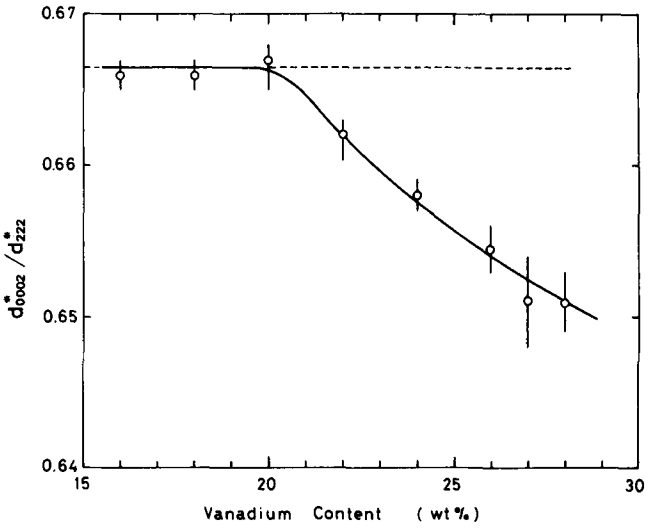

Fig. 8—Ratio of reciprocal space distance d^*_{0002} to d^*_{222} in as-quenched Ti-V alloys as a function of composition.

B. *Ti-Mo Alloys*

β phase was retained in Ti-Mo alloys containing more than 11 wt pct molybdenum. Deformation at room temperature in Ti-11, 12, 13 wt pct Mo results in {332}⟨113⟩ twinning independent of orientation of compression axis investigated, while {332}⟨113⟩ twinning or ⟨111⟩ slip appeared dependent on orientation in Ti-15 wt pct Mo. The result is shown in Figure 9, indicating that twinning is preferentially formed in orientations having large Schmid factor for $(\bar{3}32)\,[\bar{1}1\bar{3}]$. This tendency is in good agreement with the results of β Ti-V,[2] Ti-Nb,[3] and Ti-Fe[4] alloys. Figures 10(a), (b), and (c) show electron diffraction patterns obtained from the twin boundary region, matrix, and twin adjacent to the twin boundary, respectively, in deformed Ti-11 wt pct Mo. Reflections of two ω variants with equal intensity are seen in the twin. This result is similar to that of Figure 3. The similar electron diffraction patterns to Figure 10 were

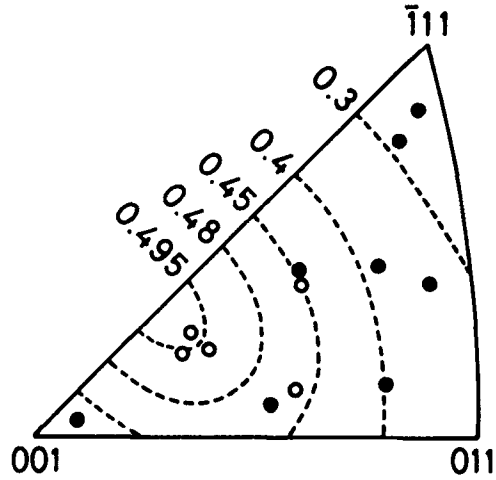

Fig. 9—Orientation dependence of plastic deformation mode in Ti-15 wt pct Mo deformed in compression. Deformation mode is {332}⟨113⟩ twinning and ⟨111⟩ slip in orientation marked by an open and solid circle, respectively. Dotted lines indicate contours with equal Schmid factor for $(\bar{3}32)\,[\bar{1}1\bar{3}]$ twinning.

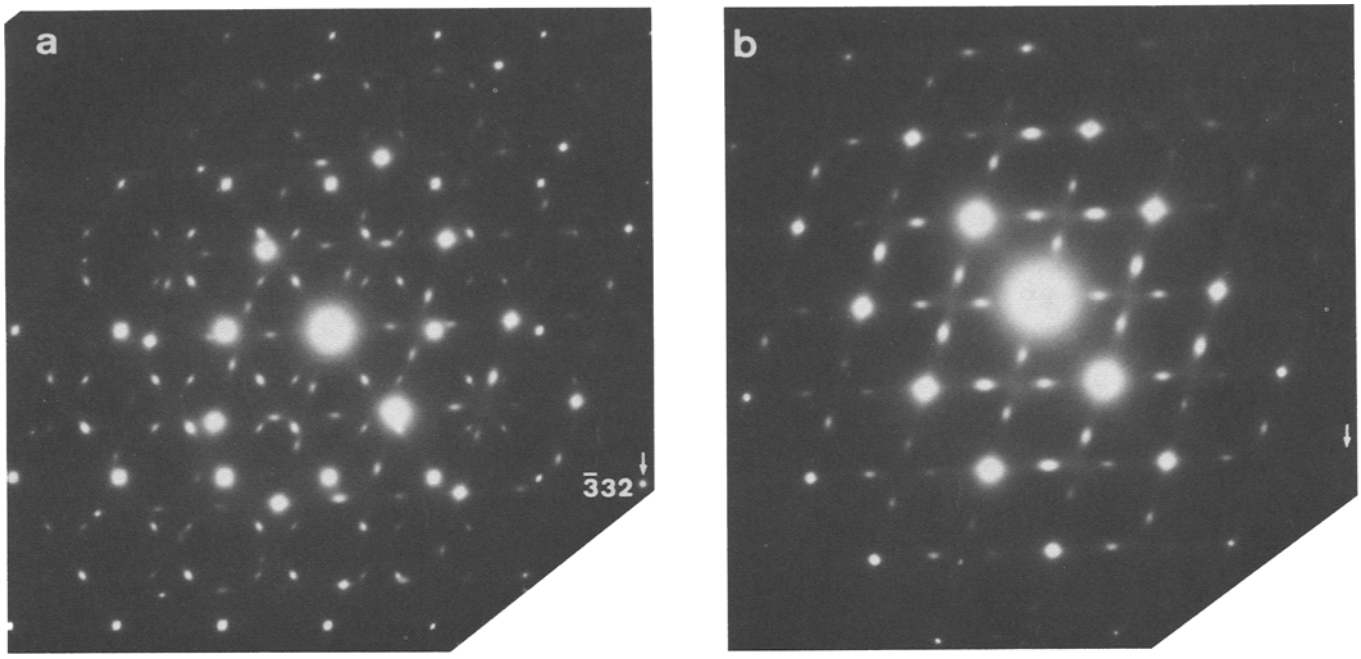

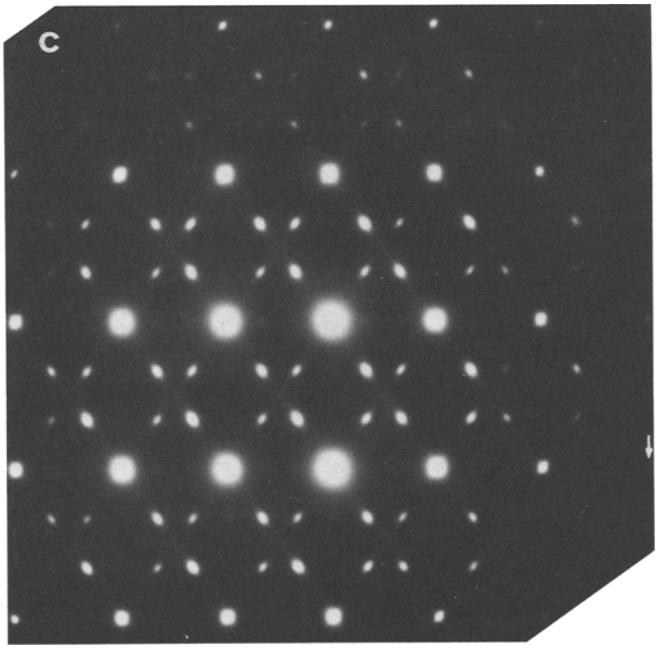

Fig. 10—Electron diffraction patterns from $(\bar{3}32)[\bar{1}1\bar{3}]$ twin boundary region (*a*), matrix (*b*), and twin (*c*) in Ti-11 wt pct Mo. The electron beam $\| [110]_\beta$.

obtained from the twin boundary region in Ti-12, 13, 15 wt pct Mo. Figure 11 shows composition dependence of d^*_{0002}/d^*_{222} obtained from β and ω reflections in the retained β phase of Ti-Mo alloys. It is apparent that the ratio is less than 0.667 throughout the investigated composition range, showing that athermal ω phase of the Ti-Mo alloys is not hexagonal. $\{332\}\langle 113\rangle$ twinning tends to occur in Ti-Mo alloys having larger ratio than 0.660 as Ti-V alloys do.

C. *Ti-Nb Alloys*

β phase of Ti-Nb alloys was completely retained in Ti-40 wt pct Nb, which was the lower limit of niobium content for the retention of β phase. $\{332\}\langle 113\rangle$ twinning or $\langle 111\rangle$ slip occurs dependent on orientation. Figures 12(a), (b), and (c) show electron diffraction patterns obtained from the twin boundary region, matrix, and twin adjacent to the twin boundary, respectively, in deformed Ti-40 wt pct Nb. This figure is quite similar to Figures 3 and 10. However, displacement of 0002 reflection is negligible (Figure 13), in contrast to Figures 8 and 11.

D. *Ti-Fe Alloys*

β phase of Ti-Fe alloys was retained in Ti-Fe alloys containing more than 4 wt pct iron. $\{332\}\langle 113\rangle$ mechanical

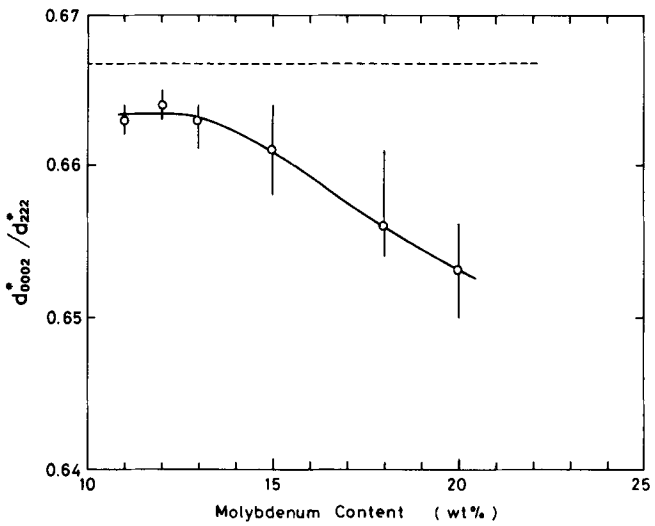

Fig. 11—Ratio of d^*_{0002}/d^*_{222} in as-quenched Ti-Mo alloys as a function of composition.

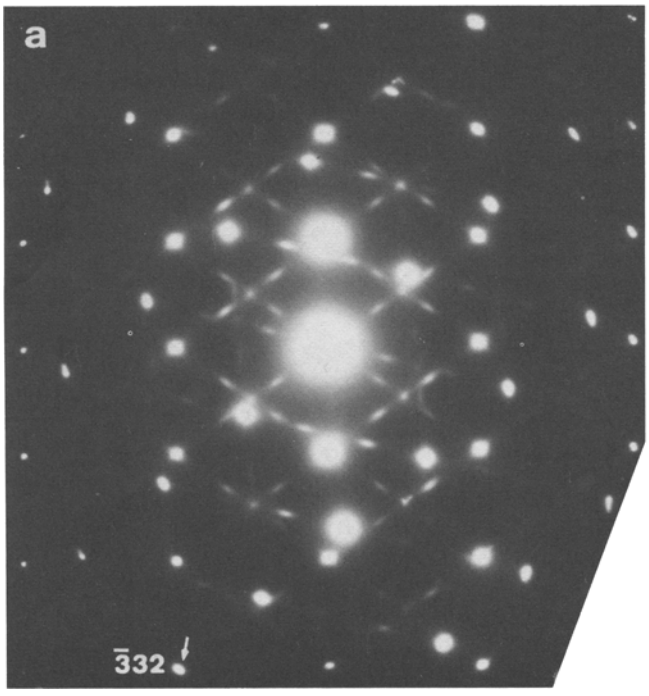

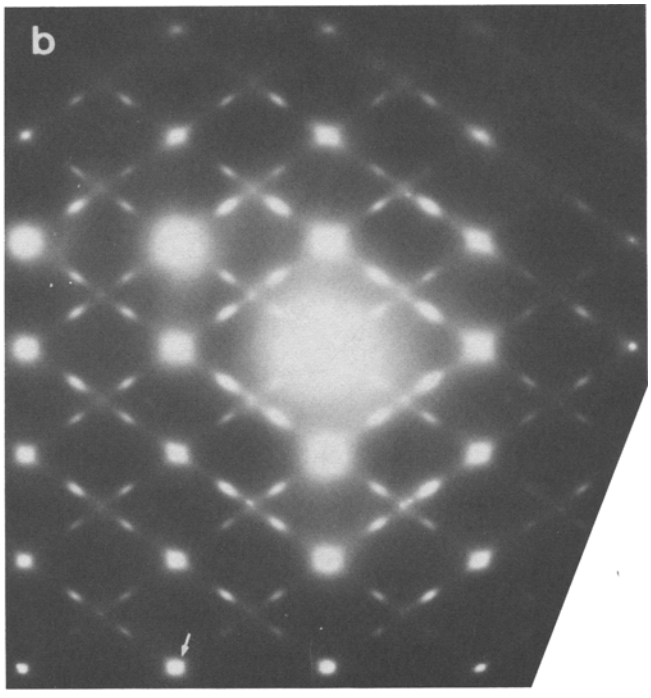

Fig. 12—Electron diffraction patterns from $(\bar{3}32)[\bar{1}\bar{1}3]$ twin boundary region (*a*), matrix (*b*), and twin (*c*) in Ti-40 wt pct Nb. The electron beam $\parallel [110]_\beta$.

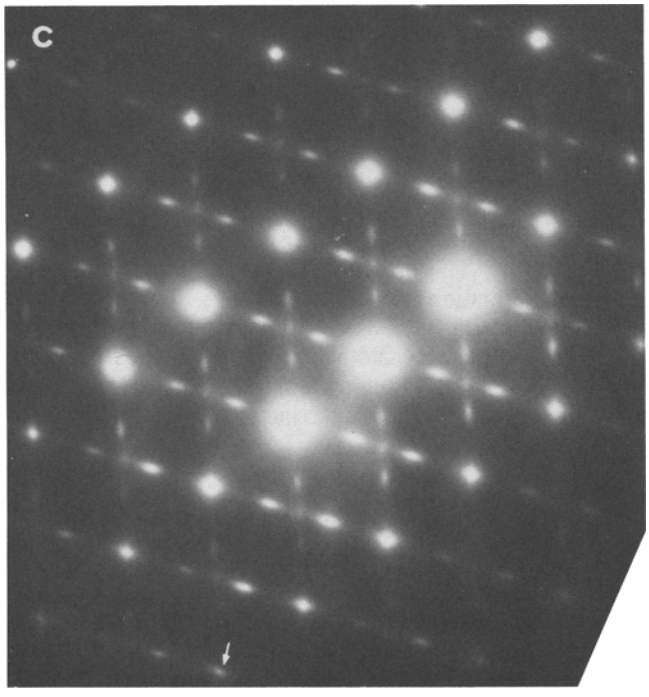

twinning in a eutectoid alloy such as Ti-Fe has been confirmed recently.[4] Figures 14(a), (b), and (c) show electron diffraction patterns obtained from the twin boundary region, matrix, and twin adjacent to the twin boundary, respectively, in deformed Ti-5 wt pct Fe. It is evident from Figure 14(c) that the two ω variants in the twin are different in intensity from each other. Especially, the intensity of the one ω variant is stronger than that of ω phase in the matrix, suggesting the occurrence of stress-induced ω phase transformation *via* $\{332\}\langle 113\rangle$ twinning. As shown in Figure 15 d^*_{0002}/d^*_{222} decreases with increasing iron content, and $\{332\}\langle 113\rangle$ twinning appears when the ratio is larger than 0.660.

IV. DISCUSSION

The obtained results in this study can be explained by the idea that stress-induced ω phase transformation in β phase titanium alloys occurs *via* $\{332\}\langle 113\rangle$ mechanical twinning. This explanation is different from that of Kuan *et al.*[8] on

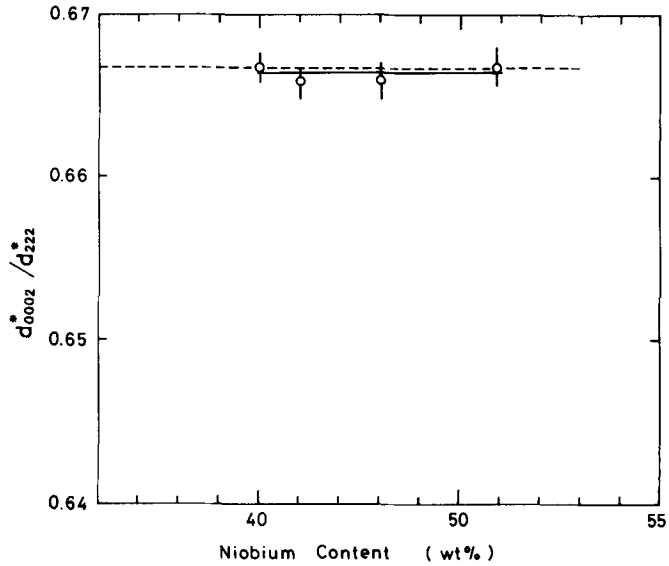

Fig. 13—Ratio of d^*_{0002}/d^*_{222} in as-quenched Ti-Nb alloys as a function of composition.

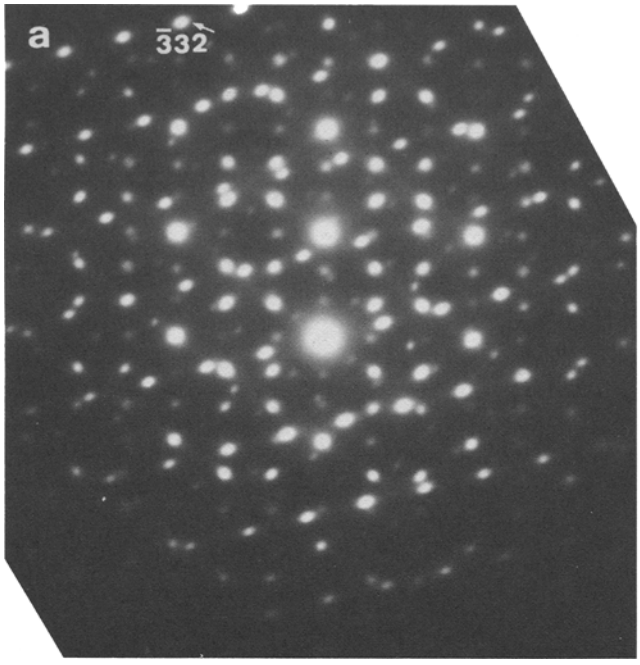

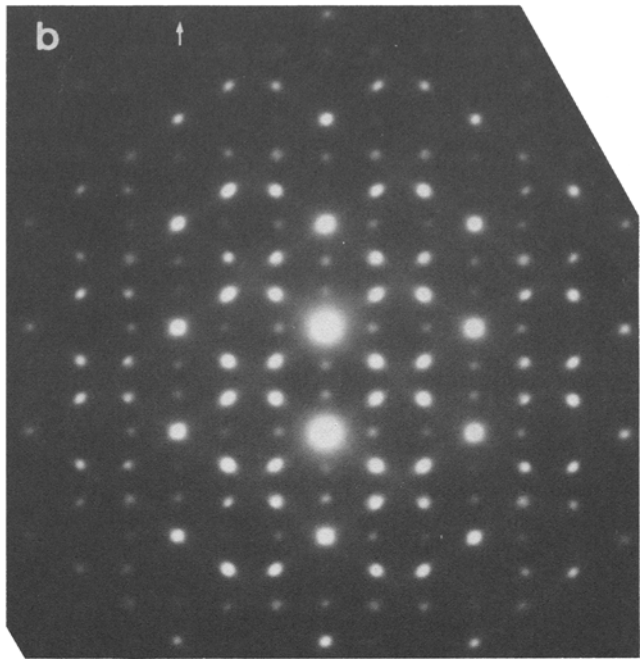

Fig. 14—Electron diffraction patterns from $(\bar{3}32)[\bar{1}1\bar{3}]$ twin boundary region (*a*), matrix (*b*), and twin (*c*) in Ti-5 wt pct Fe. The electron beam $\| [110]_\beta$.

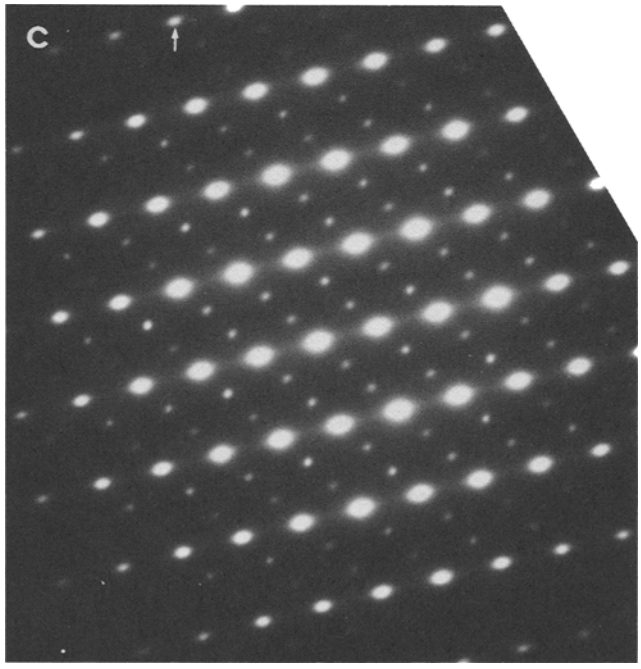

stress-induced ω phase transformation in Ti-15.8 and 20 wt pct V, although the electron diffraction pattern taken from a stress-induced plate in this study on Ti-18 wt pct V, Figure 6(c), is quite similar to that of Figure 8(c) in Reference 8. They observed stress-induced plates consisting of one ω variant, with the orientation relation to the parent β phase that $(11\bar{2}0)_\omega$ was parallel to $(110)_\beta$ and $(0001)_\omega$ was rotated 4.5 deg away from $(001)_\beta$ toward $(\bar{1}10)_\beta$. The habit plane was of the type {554}, different from mechanical twinning planes found in β phase titanium alloys such as {112} and {332}. A {332}⟨113⟩ twin possesses, however, the orientation relation to the parent β phase that $(110)_{twin}$ is parallel to $(110)_\beta$ and $(111)_{twin}$ is rotated 4.3 deg away from $(001)_\beta$ toward $(\bar{1}10)_\beta$. Therefore, the orientation relation presented by Kuan *et al.*[8] can be explained consistently in terms of stress-induced ω phase transformation *via* {332}⟨113⟩ twinning, since ω phase has well-known orientation relation to the parent β phase of $[0001]_\omega \| [111]_\beta$ and $(11\bar{2}0)_\omega \| (110)_\beta$. The present idea on the stress-induced ω phase transformation may be supported by Figure 16, where diffraction patterns were taken from a boundary region of a stress-induced plate in another foil of the same sample as Figure 6. The diffraction pattern taken from the stress-induced plate indicates two ω variants, although their reflec-

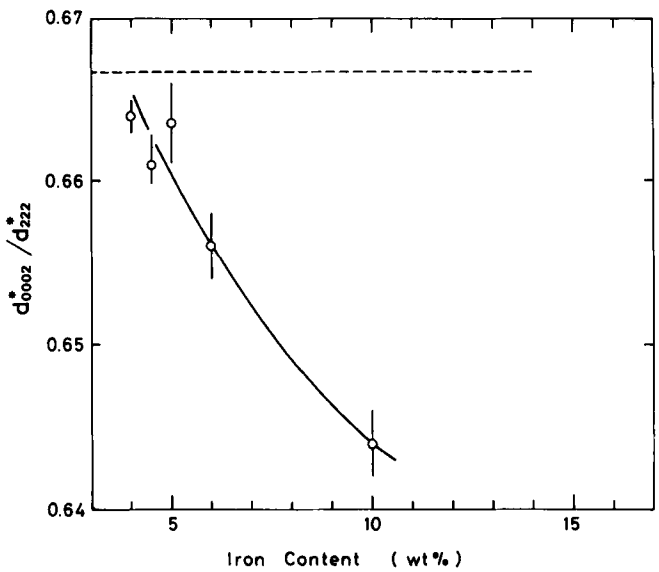

Fig. 15—Ratio of d^*_{0002}/d^*_{222} in as-quenched Ti-Fe alloys as a function of composition.

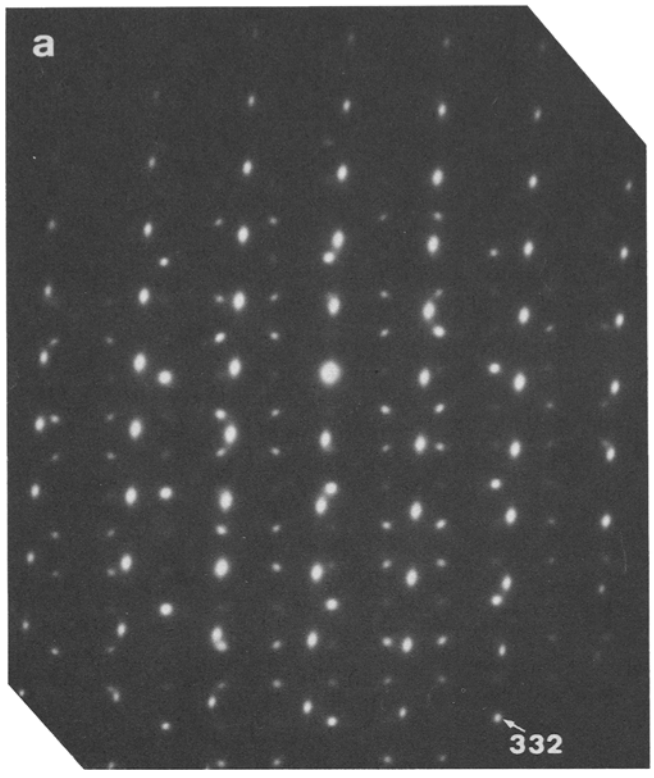

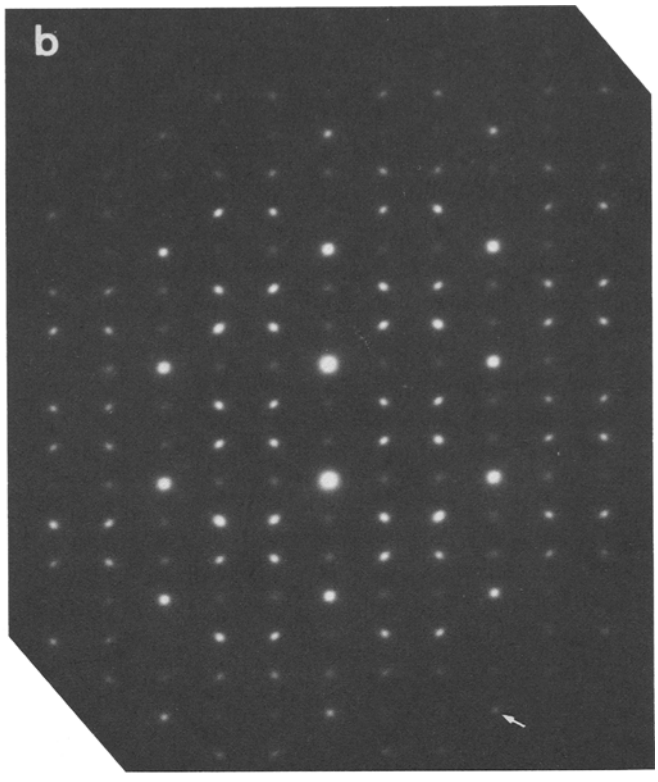

Fig. 16—Electron diffraction patterns from the boundary region of a stress-induced ω plate (*a*), matrix (*b*), and plate (*c*) in Ti-18 wt pct V. The electron beam $\| [110]_\beta$.

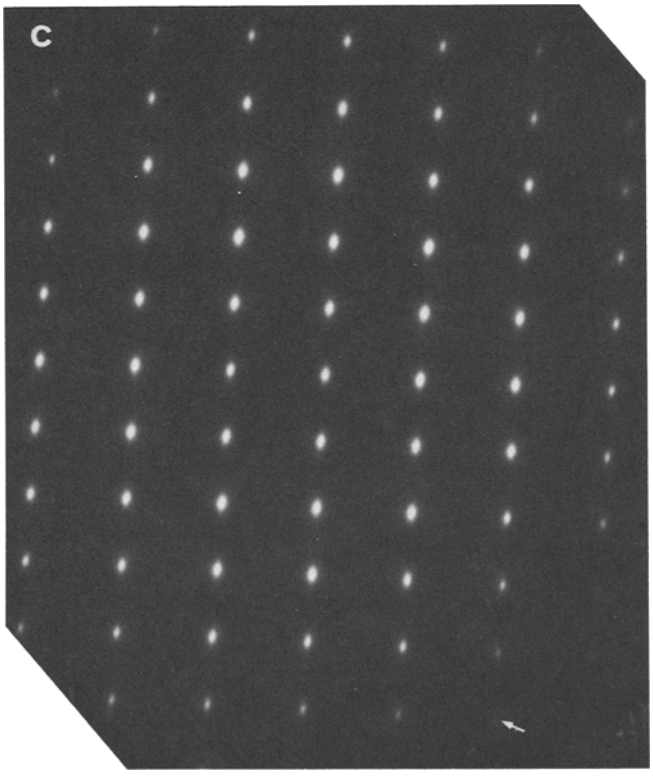

tions show marked anisotropy. These patterns are entirely consistent with Figure 4. Four ω variants are used to precipitate on aging with an equivalent density. The reason why one variant of ω phase is preferentially induced during deformation is not understood at present, but it may be related to the $\{332\}\langle 113\rangle$ shear.

Kuan *et al.*[8] further showed that there was orientation dependence of tensile axis for stress-induced ω phase transformation of Ti-15.8 wt pct V, as shown in Figure 17, where an open and solid circles correspond to orientation in which ω phase and slip were induced under tensile deformation, respectively. Recently, preferable orientation for $\{332\}\langle 113\rangle$ twinning in β phase titanium alloys has been

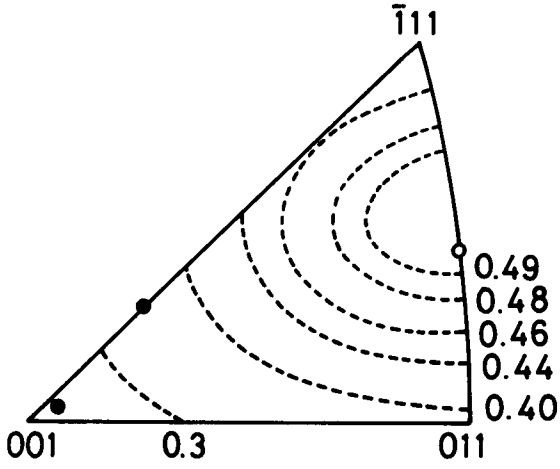

Fig. 17—Orientation dependence of plastic deformation mode in Ti-15.8 wt pct V deformed in tension after Kuan *et al.*[8] Deformation mode is stress-induced ω transformation and $\langle 111\rangle$ slip in orientation marked by an open and solid circle, respectively. Dotted lines indicate contours with equal Schmid factor for $(233)[\bar{3}11]$.

found to be controlled by both Schmid factor and polarization for $\{332\}\langle 113\rangle$ twinning.[2,3,4] The present result in Figure 9 can be also interpreted by the two factors. According to the interpretation,[2,3,4] in compressive deformation of sample having an axis in the stereographic triangle [001]-[011]-[$\bar{1}$11], the most favorable twinning system is ($\bar{3}$32)[$\bar{1}\bar{1}$3] among twelve $\{332\}\langle 113\rangle$ systems. Figure 9 shows that twinning is found in orientations with large Schmid factor for ($\bar{3}$32)[$\bar{1}\bar{1}$3]. On the other hand, on tensile deformation, (233)[$\bar{3}$11] is the most favorable twinning system. When the Schmid factor for (233)[$\bar{3}$11] is illustrated by dotted contours in Figure 17, one can recognize easily that orientation in which ω phase transformation was found by Kuan *et al.*[8] possesses the large Schmid factor for (233)[$\bar{3}$11] twinning.

The habit planes determined by Kuan *et al.* were close to {554} or {443}, while the {332} plane was observed in this study. Whether the slight difference is significant or not is uncertain at present, since many investigations[2,5,12] have shown that there is considerable scatter in habit planes of stress-induced plates in β titanium alloys. The scatter may result from the second-order twinning that distorts the original habit plane, as Blackburn and Feeney[12] pointed out.

Oka and Taniguchi[5] observed $\{332\}\langle 113\rangle$ twinning not accompanied by ω transformation in Ti-15.5 wt pct V in disagreement with Kuan *et al.* and present work. This discrepancy may be caused by the different amount of interstitial atoms such as oxygen, since Oka and Taniguchi prepared thin foils from hot rolled thin plates. According to Williams *et al.*,[13] increased oxygen content suppresses athermal ω transformation in Ti-V alloys. Therefore, oxygen may have a similar effect on stress-induced ω transformation.

d^*_{0002}/d^*_{222} of Ti-Mo in which $\{332\}\langle 113\rangle$ twinning is induced during deformation is always smaller than 0.667; see Figure 11. Correspondingly, strength of ω reflections in a twin was found to be equal to that in the adjacent matrix throughout the composition range, suggesting that ω phase transformation was not induced during deformation. This tendency is in a similar manner to Ti-22 wt pct V. However, Hida *et al.*[10] have confirmed using X-ray precession method that ω phase is induced in a twin of Ti-14 wt pct Mo deformed in tension. To check whether this difference results from direction of applied stress, *i.e.*, tension or compression, tensile tests of Ti-11, 13, 15 wt pct Mo were performed. As shown in Figure 18, the same results as compression tests were obtained on ω reflections in a twin. Displacement of d^*_{0002}/d^*_{222} from 0.667 which Hida *et al.* have shown in Figure 4 of Reference 10 seems to be smaller than that in this study. This may suggest that d^*_{0002}/d^*_{222} is dependent not only on composition but also on cooling rate from solution treatment temperature. Furthermore, the ratio was found to be influenced by heat treatment after quenching. For example, it approached 0.667 even on aging at relatively low temperature, *e.g.*, at 620 K for 600 seconds in agreement with previous work by Terauchi *et al.*[14] Nevertheless, $\{332\}\langle 113\rangle$ twinning never occurred in aged Ti-Mo.

Thus, the following conclusion may be drawn. When athermal ω phase in metastable β phase Ti-V and Ti-Mo alloys has hexagonal structure, that is, d^*_{0002}/d^*_{222} is equal to 0.667, stress-induced ω transformation occurs. As the ratio decreases, $\{332\}\langle 113\rangle$ twinning appears without stress-induced ω transformation. On further decrease of the ratio,

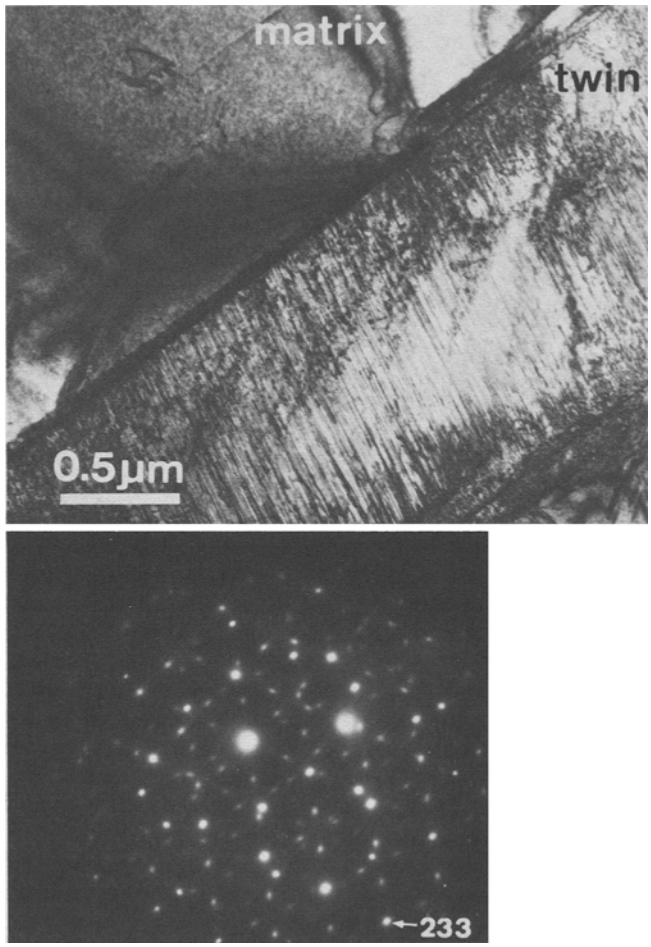

Fig. 18—Bright-field image and the corresponding electron diffraction pattern from the (233)[$\bar{3}$11] twin boundary region in Ti-13 wt pct Mo deformed in tension. The electron beam ∥ $[0\bar{1}1]_\beta$.

only slip occurs. This relationship holds true in β Ti-Fe alloys (see Figures 14 and 15). In addition, it does in commercial β phase alloys in Ti-15 wt pct Mo-5 wt pct Zr and Ti-15 wt pct Mo-5 wt pct Zr-3 wt pct Al, since d^*_{0002}/d^*_{222} of these alloys was measured in this study to be 0.663 and 0.655, respectively, and it has been reported that dominant deformation modes of these alloys are $\{332\}\langle 113\rangle$ twinning and $\langle 111\rangle$ slip, respectively.[15,16]

On the contrary, although d^*_{0002}/d^*_{222} in Ti-Nb alloys is close to 0.667 throughout the investigated composition (Figure 13), ω is not induced in a twin, as shown in Figure 12. According to Balcerzak and Sass,[17] displacement of d^*_{0002}/d^*_{222} from 0.667 becomes significant with increasing niobium content over the present composition. Therefore, the relationship between athermal ω structure and stress-induced ω transformation or plastic deformation mode for Ti-V, Ti-Mo, and Ti-Fe alloys does not hold for Ti-Nb alloys. It is noticeable, however, that Luhman and Curzon[11] have observed the formation of one variant of ω phase in deformed Ti-35.4 wt pct Nb. The specimens they used were vacuum cooled to room temperature after homogenization. Then, a vacuum cooled Ti-36 wt pct Nb alloy was deformed in compression and microstructure was investigated. The result is shown in Figure 19, indicating clearly that one ω variant is formed in a $\{332\}\langle 113\rangle$ twin

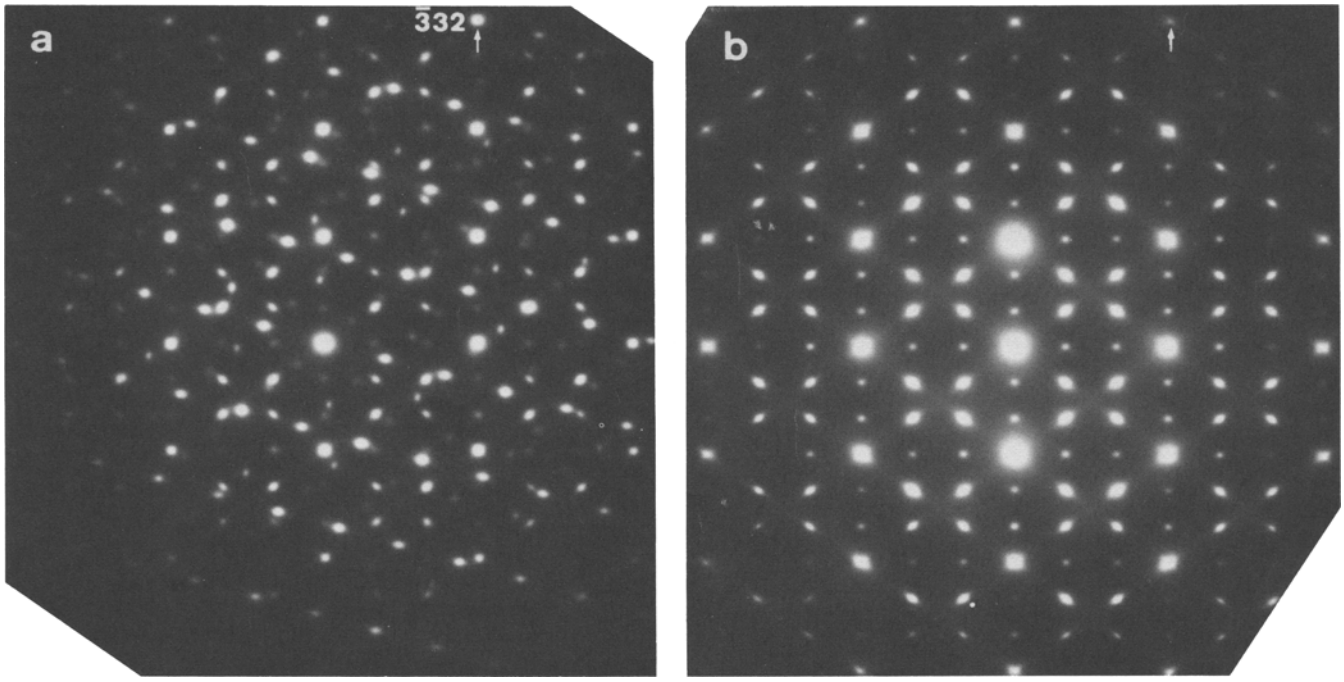

Fig. 19—Electron diffraction patterns from $(\bar{3}32)\,[\bar{1}1\bar{3}]$ twin boundary region (*a*), matrix (*b*), and twin (*c*) in vacuum cooled Ti-36 wt pct Nb. The electron beam $\| \{110\}_\beta$.

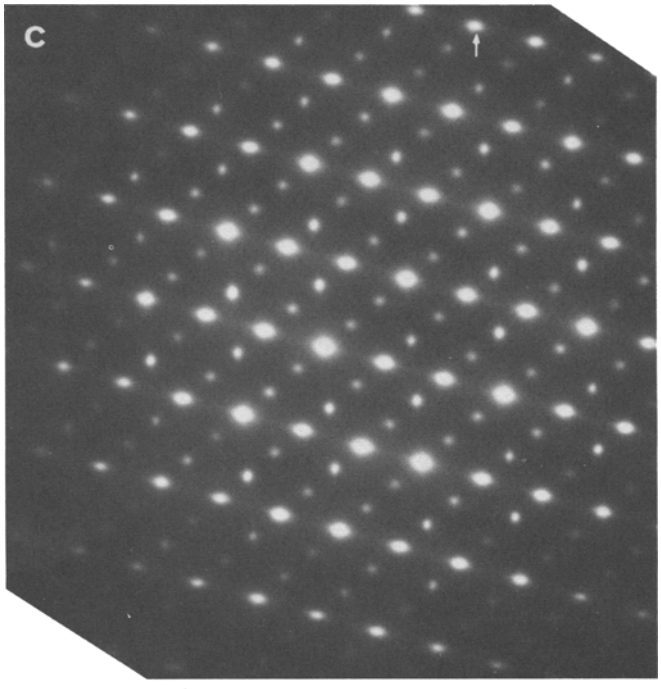

preferentially to another variant in quite similar mode to Figures 14 and 16. This observation shows that cooling rate after homogenization is sensitive to stress-induced ω transformation.

It is concluded from these observations that stress-induced ω phase transformation in β titanium alloys is related to formation of $\{332\}\langle 113\rangle$ twinning.

V. SUMMARY

A systematic study has been made of the relation between $\{332\}\langle 113\rangle$ mechanical twinning and stress-induced ω phase transformation in various metastable β titanium alloys. Stress-induced ω transformation or $\{332\}\langle 113\rangle$ twinning took place during room temperature deformation in circumstances where β phase was very unstable. Transmission electron microscopy showed that one variant of ω phase was preferentially induced in a $\{332\}\langle 113\rangle$ twin. The stress-induced ω phase transformation was influenced not only by alloy system and its composition, but also by cooling rate from solution treatment temperature. Therefore, the present results suggest that stress-induced ω transformation is related to instability of β phase or structure of athermal ω phase.

ACKNOWLEDGMENTS

The authors would like to thank A. Takemura, Kobe Steel, Ltd. for helpful discussion and Osaka Titanium Co., Ltd. for the supply of high purity titanium.

REFERENCES

1. B. S. Hickman: *J. Mater. Sci.*, 1969, vol. 4, pp. 554-63.
2. S. Hanada, A. Takemura, and O. Izumi: *Trans. Japan Inst. Metals*, 1982, vol. 23, pp. 507-17.
3. S. Hanada, M. Ozeki, and O. Izumi: *Metall. Trans. A*, 1985, vol. 16A, pp. 789-95.
4. S. Hanada, T. Yoshio, and O. Izumi: *J. Mater. Sci.*, in press.
5. M. Oka and Y. Taniguchi: *J. Japan Inst. Metals*, 1978, vol. 42, pp. 814-20.
6. A. G. Crocker: *Acta Metall.*, 1962, vol. 10, pp. 113-22.
7. Yu. A. Bagaryatskij, T. V. Tagunova, and G. I. Nosova: *Problemy Metallovedenija i Fisiki Metallov.*, 1958, vol. 5, pp. 210-16.

8. T. S. Kuan, R. R. Ahrens, and S. L. Sass: *Metall. Trans. A*, 1975, vol. 6A, pp. 1767-74.
9. R. M. Wood: *Acta Metall.*, 1963, vol. 11, pp. 907-14.
10. M. Hida, E. Sukedai, C. Henmi, K. Sakaue, and H. Terauchi: *Acta Metall.*, 1982, vol. 30, pp. 1471-79.
11. T. S. Luhman and A. E. Curzon: *J. Mater. Sci.*, 1972, vol. 7, pp. 710-12.
12. M. J. Blackburn and J. A. Feeney: *J. Inst. Metals*, 1971, vol. 99, pp. 132-34.
13. J. C. Williams, D. de Fontaine, and N. E. Paton: *Metall. Trans.*, 1973, vol. 4, pp. 2701-08.
14. H. Terauchi, K. Sakaue, and M. Hida: *J. Phys. Soc., Japan*, 1981, vol. 50, pp. 3932-36.
15. S. Hanada and O. Izumi: *Metall. Trans. A*, 1980, vol. 11A, pp. 1447-52.
16. S. Hanada and O. Izumi: *Trans. Japan Inst. Metals*, 1982, vol. 23, pp. 85-94.
17. A. T. Balcerzak and S. L. Sass: *Metall. Trans.*, 1972, vol. 3, pp. 1601-05.